**A THESIS FOR THE DEGREE OF MASTER OF SCIENCES**

# Detection of the presence of heart rots in Teak trees by stress wave method

# 응력파를 이용한 티크 내 심재 부후 탐지

By

Kyaw Ko Win

PROGRAM IN ENVIRONMENTAL MATERIALS SCIENCE

GRADUATE SCHOOL

SEOUL NATIONAL UNIVERSITY

AUGUST, 2014

# Detection of the presence of heart rots in Teak trees by stress wave method

# 응력파를 이용한 티크 내 심재 부후 탐지

**UNDER THE SUPERVISION OF ADVISOR**
**PROF. JUN-JAE LEE**

**SUBMITTED TO THE FACULTY OF THE GRADUATE SCHOOL OF SEOUL NATIONAL UNIVERSITY**

**BY**

**KYAW KO WIN**

MAJOR IN ENVIRONMENTAL MATERIALS SCIENCE
AUGUST 2014

APPROVED AS A QUALIFIED DISSERTATION OF
**KYAW KO WIN**

FOR THE DEGREE OF MASTER OF SCIENCES
BY THE EXAMINING COMMITTEE

| | | |
|---|---|---|
| **CHAIR** | **HWAN MYEONG YEO** | ---------- |
| **VICE-CHAIR** | **JUN JAE LEE** | ---------- |
| **MEMBER** | **HYUN JOONG KIM** | ---------- |

# ABSTRACT

Teak tree is famous for its strength, attractive grain pattern, resistance to termites, its durability and pleasant color. Over the past decades, teak natural forests in Myanmar have been degraded because of extraction of timber to export to foreign countries, illegal logging and extensive requirement of timber because of population pressures. Myanmar Government has planned and implemented to establish teak plantations throughout the country to get sustainable supply of desirable amount and quality of timber from teak plantation without increasing pressure on natural teak forests.

Thinning operation is necessary for successful teak plantation. By eliminating some trees from a plantation, the remaining trees can get more sunlight, nutrient and reducing competition among them. Wrongly choosing sound trees to fell and leaving defective trees will lead to a great economic loss. Visual inspection cannot detect the defects located inside tree trunks like heart rots. Although the existing stress wave CT instruments provide a tree cross-section with tomograph, a deep experience is necessary to correctly decide tree condition by interpreting the images. To avoid wrong decision-making, additional criteria were required to decide the presence of defect. The purpose of this study was to develop criteria to determine the presence of heart rots in teak trees.

When stress wave CT imaging instrument is used to inspect trees, transducers are mounted around the circumference of tree stem. Transducer numbers 8, 10 and 12 were used to measure the time of flight among transducers. The angles among transducers were measured on the basis of a straight baseline (180˚) in a cross-section. The angles among 8, 10 and 12 transducers were (45˚, 90˚, 135˚ and 180˚), (36˚, 72˚, 108˚, 144˚, and 180˚) and (30˚, 60˚, 90˚, 120˚, 150˚ and 180˚) respectively. To develop reference velocity for each transducer angle, 25 sound discs were used. As heart rot forms near the centre of a tree stem, the cross-section was distinguished into two parts; outer zone and inner zone based on transducers' angles. Outer zone includes angles smaller and equal to 90˚ and inner zone includes angles larger than 90˚.

The result defines that the velocity of outer zone is slower than that of inner zone in 25 sound discs. This is because the smaller angles (≤90˚) are closely oriented with the annual rings in tangential direction and the larger angles are nearer to radial direction. Firstly, analysis of the average velocities of inner zone with outer zone was carried out on referenced 25 sound discs. ADV (Average Difference Velocity %) between these two zones of each disc with each transducer number was calculated. The reference mean ADV indices of 25 sound discs were determined (-6.26%, -9.53% and -8.35%) for 8, 10 and 12 transducers relatively.

Same experimental measurements on 10 sound discs and 9 heart-rot discs were done. The ADVs of 10 sound discs range from (-8.61% ~ -15.25%), (-5.7% ~ -11.62%) and (-6.97% ~ -15.94%) for 8, 10 and 12 transducers. The ADVs of 9

heart-rot discs range from (10.68% ~ -8.38%), (14.2% ~ -5.26%) and (9.93% ~ -7.4%) for 8, 10 and 12 transducers. Since heart rots locate in the inner zone of cross-section, the average velocity of outer zone is not much slower or even faster than that of inner zone's average velocity in defective discs. The resulted ADVs of 19 tested discs were compared with reference ADV indices. The result indicated that ADV indices could successfully distinguish sound and heart-rot discs with high accuracy (89.5 ~ 100%).

Secondly, the measured velocities of 10 sound and 9 heart-rot discs were compared with reference velocity at each transducer angle. The DIVs (Dissimilarity in Velocity) were calculated for each disc. Based on average ± DIVs of all angles and of only inner zone's angles of 19 tested discs, calibration was performed to distinguish sound and heart-rot discs. Although the accuracy (59.1 ~ 63.6%) of DIV indices did not reach satisfactory level, a linear relationship between heart-rot area ratios of defective discs and their calculated DIVs was found. This study concludes that the developed indices can be used as decision-making criteria to detect heart rots and to predict their area ratios while using the stress wave CT imaging instruments.

**Keywords:** teak plantation, thinning, heart rots, stress wave CT, average velocity difference, dissimilarity in velocity, reference velocity.

**Student number: 2012-23991**

# Table of contents

# List of figures

# List of tables

# 1. INTRODUCTION

## 1.1 Background

Myanmar is a country endowed with variety of tree species throughout the country. Myanmar has a forest cover of about 33 million ha covering nearly half of its total land surface area in 1989 (Soe, 2009). The forest cover is constituted mainly of natural forests and about half of which are teak growing forests (Kyaw, 2003). Although forest resources have been scientifically managed since 1856, they are degrading gradually both in extent and quality due to increased population pressure and continuous rising demands for timber for domestic and foreign uses. Myanmar is only one country which exports timber to foreign country and about 90% of the total amount is derived from teak (Htun and Hlaing, 2001). Annual production of teak is estimated to be about 450,000 $m^3$ (1991-2000 average) in the form of logs and sawn timbers, of which are mostly from natural forests (Kyaw, 2003). To compensate the gradual loss of teak forest from forested area, government afforded to establish teak plantation throughout the country. Teak plantations have been established on both degraded forests and depleted lands to recover forests and for sustainable use of timber for the future. Starting from early 1970s, block plantations were established in the areas with degraded forests and poor stocking of teak and other valuable commercial species (Gyi, 1972).The main objective of teak plantations establishment is to produce high quality timber in tree with good or acceptable growth rates. The total teak plantation area is shown in Figure 1.

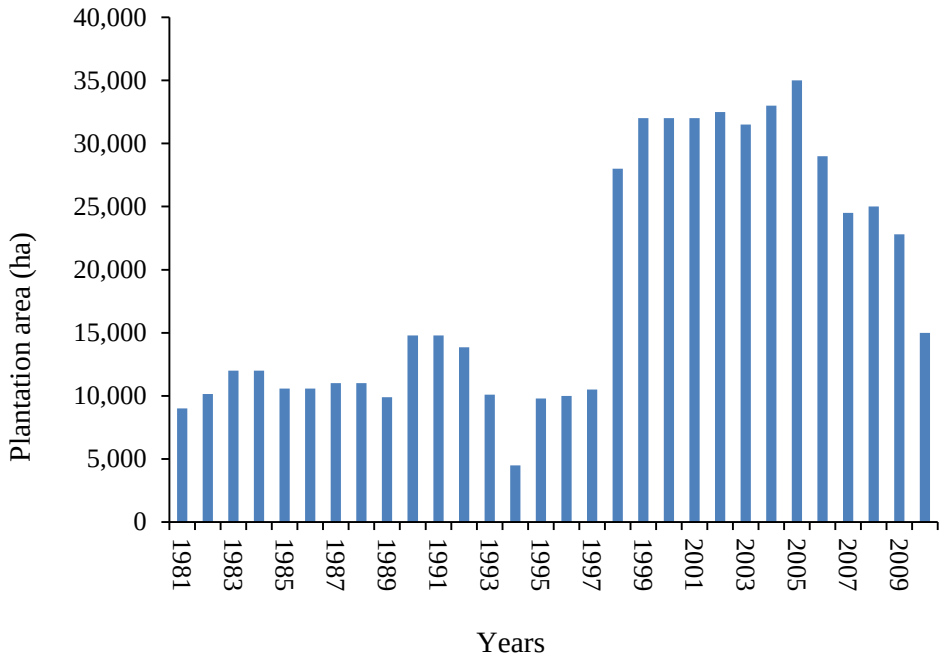


Figure 1. Establishment of Teak plantations in Myanmar (1981-2010)

(*Source: FD, 2011*)

Teak is a light demanding tree species in nature. Getting favorable conditions of lights, nutrients and soil types are some important factors affecting the high growth rate, bole straight and high quality logs from teak plantations. There are some silvicultural treatments applied to teak plantations to receive desirable quality timber. Pruning, weeding and thinning operations are some important silvicultural practices carried out in teak plantations. Pruning is cutting the branches of plantation to prevent forming knots on the wood. Weeding operation is cleaning the existing weed on the ground near the plantation trees to provide more nutrients for

them. Thinning operation is the removal of some plantation trees from a plantation to reduce the strong competition among trees and to provide more light and more nutrition for the remaining trees. For a plantation with 9ft*9ft spacing, first mechanical thinning is carried out at average height of 7.5-9 m or about 4-7 years old. About 50% of trees are thinned out alternately. Second mechanical thinning is operated at average height of 12-14 m or about 8-11 years old. About 50% of total trees are thinned again by removing trees in alternate rows. Final heavy thinning is done at age of around 40 years. After the final heavy thinning, the remaining trees are allowed to grow until they are harvested.

The major defects in teak plantation trees include knots, splitting and heart rots. Heart rots, in most case, forming in the central part of the cross-section severely degrade the quality of logs. In thinning operation, large amount of teak trees are cut to provide better environment for the remaining trees. These thinning operations are usually carried by visual inspection to choose the trees to be felled. Visual inspection may see the defects forming on the tree trunks. However, this inspection cannot recognize heart rots because they generally form within the central zone of cross-section of tree stem. In the first and second thinning, choosing the trees to be removed is easy for a tree inspector because the size of tree is small, trees are young and most of them are free from defect and if exist, they are easily remarkable. But in final heavy thinning, the trees are around 40 years old, and there is a high possibility in tree stems to have defects. As mentioned earlier, the main objective of plantation establishment is to get high quality timber. If a tree inspector wrongly chooses the sound trees to be cut and defective trees to be allowed to grow, there

will have a great loss in not only economic benefit but also getting high quality timber when they are harvested.

Stress wave method is a well-established technique for nondestructively evaluating the mechanical properties and characterizing natural defects of various wood products (Pellerin and Ross 2002). Recent research development showed a very good potential for stress wave technique to be used to assess wood quality of living trees (Wang *et al*. 2007). The presence of decay in cross-section of wood can significantly reduce the speed of a stress wave. Generally, stress waves propagate quickly through dense, solid materials, while voids, cracks, or decay attenuate and divert stress waves since the waves must find a path around the defects resulting in increased transmission times (Dackermann *et al*. 2013). A useful way to detect decays is comparison to the reference speed of sound trees. By comparing with the reference speed of defect-free tree, the location and presence of decay in wood can be detected. The speed of stress wave can be different depending on tree species because of the different wood properties in different tree species such as density, moisture content, etc. Thus, it is required to establish a specific reference speed for each tree species. There is no research on the establishment of reference speed of sound teak tree species.

There are some commercial stress wave CT (computed tomography) instruments in the market such as Fakoop, PiCUS Sonic instruments to inspect the cross-section of the tree stem. They can provide the cross-section view of the stem with computed images. The resolution of images obtained by stress wave based acoustic

tomography depends on the number of transducers used, acoustic wave frequency, and the applied evaluation algorithm. The resolution of the image is better if the applied frequency is higher, the number of sensor is higher and the applied algorithm is more advanced (Divos *et al*. 2006).

Although acoustic tomography was effective in locating defect positions, it tended to under represent decay and hole's size. Moreover, acoustic tomography could not distinguish decay or holes when only based on color change (Liang *et al* .2012). The manufacture of these CT instruments cannot guarantee the accuracy of their measurements. Moreover, a tree inspector must know clearly what the reason is for the defect that could be seen in the tomograph with various colors. Non-professional inspector can misinterpret the CT images in the field because it needs deep technical knowledge background on it. Without a suitable criterion to decide the tree has heart rot or not, a tree inspector needed to use to decide it by his own experience. Therefore, there is still limitation to use these instruments for non-professional labors.

## 1.2. Objective

The objective of this study was to develop less complex indices which could be additionally considered to determine the presence of heart rots in teak plantation trees while using CT instruments.

## 2. LITERATURE REVIEW

Various techniques, based on different concepts, have been used to detect deterioration in trees. The condition assessment of wood can be made by using various techniques such as X-ray computed tomography, ultrasonic and stress wave technologies. Stress wave and ultrasonic techniques are simpler and less costly than imaging techniques like X-ray and neutron radiography.

The use of stress waves (ultrasound or sound waves) to detect decay in trees has been explored by many researchers (Yamamoto *et al*. 1998; Wang et *al*. 2004). The concept of detecting decay using this method is based on the observation that stress wave propagation is sensitive to the presence of degradation in wood. In general terms, stress waves travel slower in decayed or deteriorated wood than sound wood. They also travel around hollows, increasing the transmission time between two testing points (Wang *et al*. 2008).

Some studies have investigated the feasibility of using stress waves in the radial direction to evaluate stem defects (Yamamoto *et al*. 1998, Wang *et al*. 2004). S. Liang *et al*. (2010) studied the various factors and propagation trends of stress waves in cross-sections of wood to improve accuracy in decay detection in standing trees by wood discs. He found that the stress wave velocity gradually decreased when the test angle changed from a radial direction to a tangential direction. Li *et al* (2013) investigated on the velocity pattern from radial to tangential direction in cross-section of Black Cherry trees. He concluded that the velocity patterns from radial to tangential direction of sound cross-sections could be used to detect internal

decay of live defective trees. The acoustic behavior of wood in the stem transverse section is a complex phenomenon. The propagation stress wave velocity showed high variability and dependency on the rotation angle of the material in the transverse section. The velocity decreases as the orientation angle increases (Dikrallah *et al.* 2010).

Since timber is inhomogeneous in nature, the grain orientation influences the speed of stress wave travel. The wave can travel through the cross-section of a tree stem in three directions; radially (perpendicular to the growth rings), tangentially (parallel to the growth rings) and across the rings at an angle between 0 and 90 degrees (Wang *et al.* 2004). The fastest is in the radial direction; stress wave speed is about 30% faster than that in other directions. These findings were resulted on the basis of the orientation between stress wave paths and the annual rings.

In case of inspecting trees, the annual ring angles orientation with stress wave paths cannot be investigated because the pith location is inconsistent inside the tree. When applied stress wave CT instruments to inspect trees, the angles between transducers which are mounted on the trunk of a tree can be known. Stress wave velocity can change according to the angles between transducers because of the anisotropic properties of wood. Therefore, it is reasonable to investigate on the transducers' angles and their related stress wave velocities.

Several types of equipments, such as the Fakopp Microsecond Timer and the Arbotom and Picus Sonic Tomographs, have been used to inspect wood for defects that might affect velocity change or tomogram presentation (Divos *et al.* 2005, Wang *et al.* 2007). The resolution of images obtained by stress wave based acoustic

tomography depends on some factors. The resolution of the image is better if the applied frequency is higher, the number of transducers is higher and the applied algorithm is more advanced (Divos *et al.* 2006). These instruments need to be understood regarding the stress waves propagation, velocity changes in different test conditions such as number of transducers, angle between two transducers, defect types and dimension. (Liang *et al.* 2010).

Li and others (2000) investigated on the effect of transducer quantity to detect log inner defects using stress wave. The results showed that for logs with diameter ranging from 20 to 40 cm; at least 12 transducers were needed to meet the requirement which ensure a high testing accuracy of roughly 90% of fitness with 0.1 of error rate. To locate the defects, 10 transducers were recommended and to decide whether there were defects or not, 6 transducers were sufficient.

Stress wave propagating perpendicular to grain is affected by tree species. To account for species difference, Divos *et al* (2002) established some reference velocities for some species for tree evaluation. Comparing with the reference velocity of a certain tree species is a useful way to inspect the internal condition of standing trees. Tallavo *et al* (2012) presented a new methodology based on theoretical, numerical and experimental studies for condition assessment of wood poles using ultrasonic tests. For each transmitter location, an array of five receivers at different angles from the transmitter is used to measure the response of the wood pole to the ultrasonic excitation. Laboratory results show that for an area of decay of 30% of the cross-section, the wave velocity and the transmission factor decrease by

51% and 96% respectively. The presence of decay in cross-section of wood can significantly reduce the speed of a stress wave. By comparing with the reference speed of defect-free wood, the location and presence of decay in wood can be detected.

# 3. MATERIALS AND METHODS

## 3.1 Materials

### 3.1.1 Specimens

Forty four Teak (*Tectona grandis* Linn.f) trees were selected from a plantation situated at Coupe no.41, Western Mone Reserved Forest at Minbu District, Magway Division in Myanmar (Figure2). The plantation trees were 41 years old. The selected trees were felled at 30 cm from the ground surface. The cross-sections of the felled trees were visually checked. A disc was sliced from each tree stem by a chain-saw at a height of 30 cm from the base of the stem. Those forty four Teak discs were wrapped by plastic bags immediately after being felled to prevent them from being dried. The sizes of these discs were ranging from 200-300 mm in diameter and irregular in shape. Among them, nine discs had heart rots with various sizes near the central zones of the cross sections. Those discs were transported to Korea by shipment. After receiving them at Seoul National University, they were kept in a refrigerator with plastic wrapping.

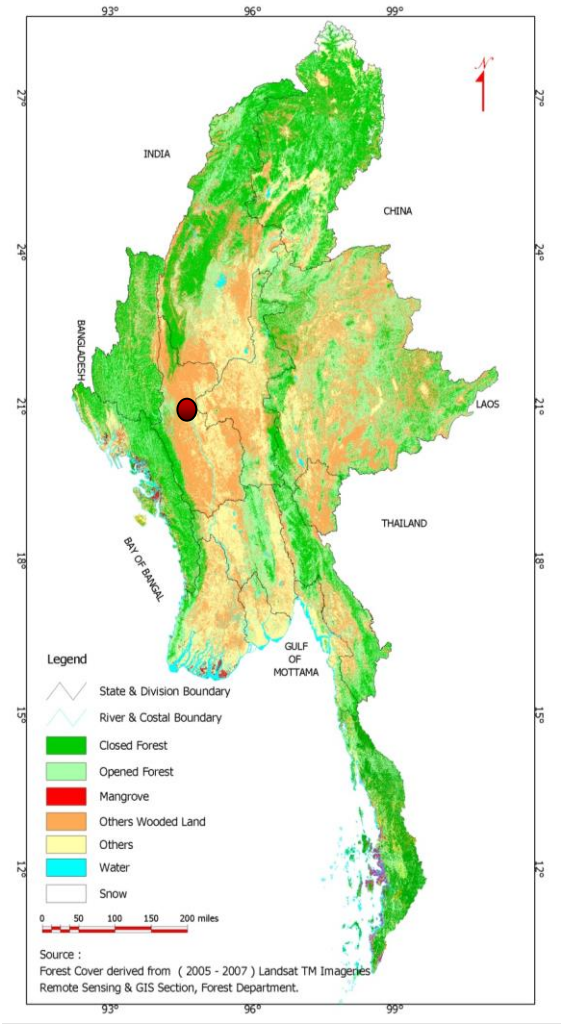


Figure 2. The location map of teak plantation at Minbu township in Myanmar

*Source: Forest Cover Status of Myanmar (FRA, 2010)*

## 3.2. Methods

### 3.2.1. Experimental set ups and velocity calculation

A PiCUS Sonic Tomograph (Version 3) instrument was used for stress wave travel time measurement. In PiCUS Sonic Tomograph and there are 12 transducers with cable loom and an impact hammer (Figure 3-a). A disc was unpacked from the plastic bags and weighed. The measuring points were made to locate the positions of transducers around the circumference of a disc. The locations of the points on the cross-section (from A to H) for 8 transducers test set up and the wave paths from transmitting transducer to receiving transducers were shown in Figure 3-b. The nails were driven at those points and the transducers were attached to these nails. The experimental setup of transducers on the disc and the angles between transducers for 8 transducers set up (Figure 3-c). The angle Ɵ is the angle between transmitter and related receiver. The receivers were set at the receiver angles Ɵ=45˚, Ɵ=90˚, Ɵ=135˚ and Ɵ =180˚. The travel time was measured by tapping five times on transmitter A with an impact hammer. The stress wave, released from transmitting transducer A, was received by 7 receiving transducers (B, C, D, E, F, G and H) and measured the travel times from a transmitter to all receivers. The next tapping was carried out on B transmitter and the other 7 receivers (C, D, E, F, G, H and A) captured the wave from B and recorded the travel time. The same process continued until all the transducers had been tapped five times per each alternately. In this study, three test setups with 8, 10 and 12 numbers of transducers were used. The same procedure was also done for 10 and 12 transducers (Figure 4-a, and 4-b). After

carried out the testing, the number of transducers and their related angles between transducers were tabled as described in Table 1.

(a)

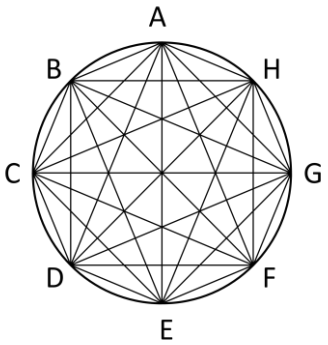


(b)

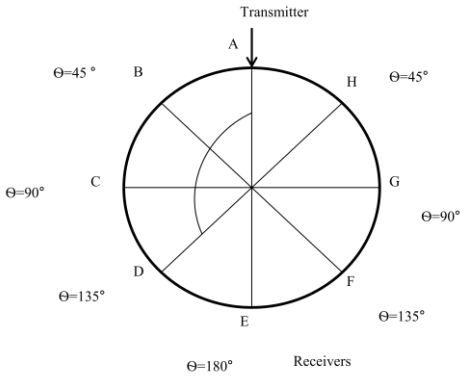


(c)

Figure 3. PiCUS Sonic Tomograph (a), stress wave paths passing through the cross-section (b), experimental set up of transducers on the circumference with 8 transducers (c).

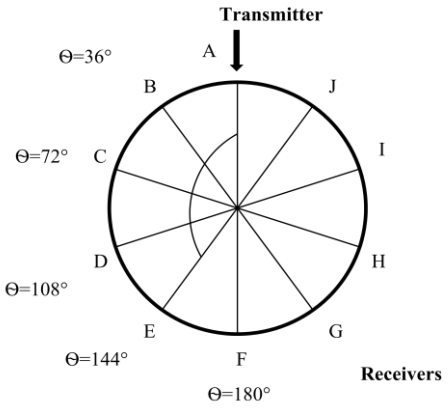


(a)

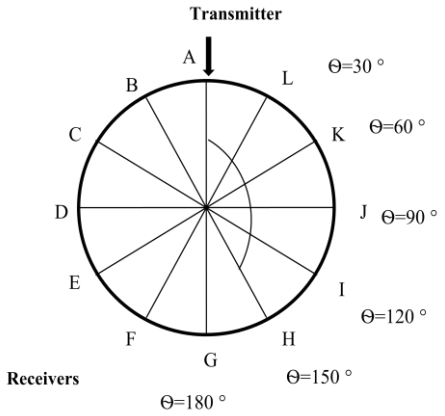


(b)

Figure 4. Experimental set up of transducers on the circumference and angles between them with (a) 10 transducers and (b) 12 transducers.

Table 1. Number of transducers and the angles between transducers for one disc

| Number of transducers | Angles between transducers |
|---|---|
| 8 | 45˚, 90˚, 135˚, 180˚ |
| 10 | 36˚, 72˚, 108˚, 144˚, 180˚ |
| 12 | 30˚, 60˚, 90˚, 120˚, 150˚, 180˚ |

To investigate on the velocities of various transducers' angle orientations, twenty five sound discs were tested. Five impacts were released at each transmitting transducer and the resulting Time-Of-Flight (TOF) were recorded and downloaded to a personal computer. The velocity was calculated for each wave path by dividing the distance between a transmitter and a receiver by the travel time (Equation 1).

$$V_{\Theta} = \frac{D}{T} \qquad (1)$$

Where,

$V_{\Theta}$ is the velocity of the wave path at angle $\Theta$ from one transducer to other transducer

$\Theta$ is the angle between a transmitter and a receiver

$D$ is the distance between those two transducers

$T$ is the travel time of stress wave between those two transducers

### 3.2.2. Reference velocity development

The presence of decay in the cross-section of wood can reduce the stress wave velocity when the wave path passes the decay. Comparing the velocities of defective wood and sound wood of the same species is an effective way to detect the presence of decay in a cross-section.

25 sound discs velocities were used as the reference velocity data for sound discs (Table2). The calculated velocity data were categorized according to the angles between transducers. The mean velocity and standard deviation of each angle were calculated.

Table 2. Discs used for reference mean velocity for sound discs and discs for validation

| Discs used | Total | Sound discs | Unsound discs |
|---|---|---|---|
| | 44 | 35 | 9 |
| For reference velocity | 25 | 25 | - |
| For validation | 19 | 10 | 9 |

### 3.2.3. Indices development

In this study, attempts were made to detect heart rots by two methods;

a. Comparison of velocity difference within a cross-section (ADV method)
b. Comparison of tested discs' velocity with the reference velocity (DIV method)

#### 3.2.3.1. Comparison of average difference velocity (ADV) within a cross-section

When a stress wave was released from a transmitting transducer, it passed through the cross-section of a stem in various directions. Some wave paths were passing through the central or near the central part of the cross-section and the others were passing through the outer part as shown in Figure 5-a and 5-b. As interest was made to detect heart rots, the central part of the cross-section of a tree stem needed to be more emphasized. For that reason, the angles of the wave paths between transducers

were regrouped into two zones; inner zone angles “A-angles” and outer zone angles “B-angles”. A-angles include angles larger than 90˚, and B-angles include angles equal to and smaller than 90˚. The A-angles represent the inner part of the cross-section and the B-angles represent the outer part of the cross-section as seen in Figure 5-b. Since different experimental set ups were used with three different transducers numbers, their A and B angles according to the number of transducers were described in Table 3.

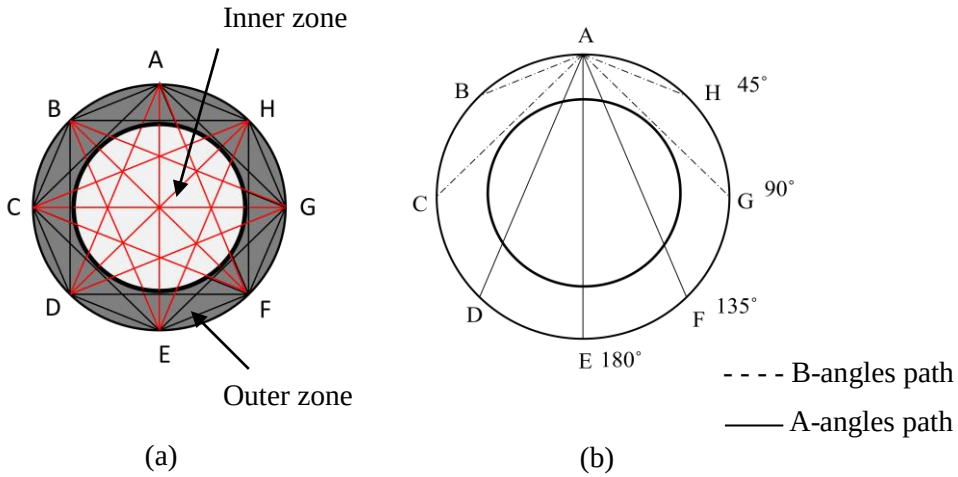


Figure 5. For 8 transducers experimental set up, Distinguishing inner zone and outer zone within a cross-section (a), “A” and “B” angles’ wave paths in the cross-section of a disc.

Table 3. Grouping angles according to their wave paths

| No. of transducers | B-angles | A-angles |
|---|---|---|
| 8 | 45˚, 90˚ | 135˚, 180˚ |
| 10 | 36˚, 72˚ | 108˚, 144˚, 180˚ |
| 12 | 30˚, 60˚, 90˚ | 120˚, 150˚, 180˚ |

Most of the stress wave paths at the smaller angles (B-angles) were considerably orientated with the annual rings in tangential directions but the orientation of most paths at the larger angles (A-angles) with the annual rings was nearer to radial directions. In general, a stress wave travels faster in radial direction than in tangential direction. By comparing the average velocity of all A-angles and B-angles for each number of transducers (8, 10 and 12), the average difference velocity (ADV) percentage could be calculated for sound and unsound discs by Equation 2.

$$ADV = \frac{V_{b(avg)} - V_{a(avg)}}{V_{a(avg)}} \times 100\% \qquad (2)$$

Where,

*ADV* is the average difference velocity percentage between "B" and "A" angles for one disc.

$V_{b(avg)}$ is the average velocity of all the "B" angles in a cross-section

$V_{a(avg)}$ is the average velocity of all the "A" angles in a cross-section

Ten sound discs and nine heart rots discs were classified into two as sound discs and defective discs. Each disk was tested with the same experimental method, calculated the velocities for each angle and averaged. Each disk's "A" angles and "B" angles' velocities were calculated and averaged. Then, the ADV was calculated for each transducer number by comparing average angles' velocities of groups "B" and "A" by using the Equation 2 for each disk. After the ADV calculations for sound and heart rot discs, indices were established by calibrating on the ADV values of discs with the different transducer numbers (8, 10 and 12).

### 3.2.3.2. Comparison of tested discs' velocity with the reference velocity (DIV)

Ten sound discs and nine heart rots discs were tested with the same experimental set up and method to get velocity measurements at different angles between transducers.

The tested discs' velocities were compared with the reference velocities for each angle for each disc by the following Equation 3.

$$DIV_{\theta} = \frac{V_{\theta} - \mu_{\theta}}{\sigma_{\theta}} \qquad (3)$$

Where,

$DIV_{\theta}$ is the dissimilarity in velocity of measured velocity compared with reference velocity for the θ angle.

θ is the angle between two transducers.

$V_{\theta}$ is the measured stress wave velocity in sound discs and defected discs for a receiver located at θ angle.

$\mu_{\theta}$ is the mean velocity of sound reference specimens at the angle θ.

$\sigma_{\theta}$ is the standard deviation for the sonic velocity of sound reference specimens at the angle θ

Dissimilarity shows how much the measured velocity at an angle differs from the reference velocity of sound discs at the same angle with the consideration of

standard deviation. The calculated dissimilarity at an angle would have negative value (<0) if the measured velocity was slower than the reference mean velocity at the same angle. Likewise, its value would be positive (>0) if the measured velocity was faster than mean velocity of reference sound discs. The dissimilarities (DIVs) for each disc were listed according to their related transducers' angles. In case of using 8 transducers, 56 DIVs were obtained for one disc. For 10 and 12 transducer numbers, 90 and 132 DIVs were obtained respectively. Based on these DIVs, four indices were developed to detect heart rots by using the following equation (3);

$$DI_{m,n} = \frac{\sum DIV_{m,n}}{n_{m,n}} \qquad (3)$$

where,

$DI_{m,n}$ is the calculated index with *m* and *n* conditions.

$DIV_{m,n}$ is the calculated dissimilarity in velocity with *m* and *n* conditions.

$n_{m,n}$ is the number of all dissimilarities of one disc with *m* and *n* conditions.

*m*;

if *m* is "*a*", $DIV_{m,n}$ and $n_{m,n}$ shall contain both angle A and angle B.

if *m* is "*i*", $DIV_{m,n}$ and $n_{m,n}$ shall contain angle A (inner zone) only.

*n*;

if *n* is "*a*", $DIV_{m,n}$ and $n_{m,n}$ shall contain both positive and negative $DIV_{m,n}$.

if *n* is "*n*", $DIV_{m,n}$ and $n_{m,n}$ shall contain negative $DIV_{m,n}$ only.

Four attempts were made to distinguish sound and heart-rot discs. First index ($DI_{a,a}$), all DIVs of all angles in a cross-section were averaged. Second index ($DI_{a,n}$), the negative DIVs of all angles were averaged. Third index ($DI_{i,a}$), all DIVs of only A angles were averaged. The fourth index ($DI_{i,n}$) was made by averaging only negative DIVs of only A angles.

## 4. RESULTS AND DISCUSSIONS

### 4.1. Reference velocity development according to transducer' angles

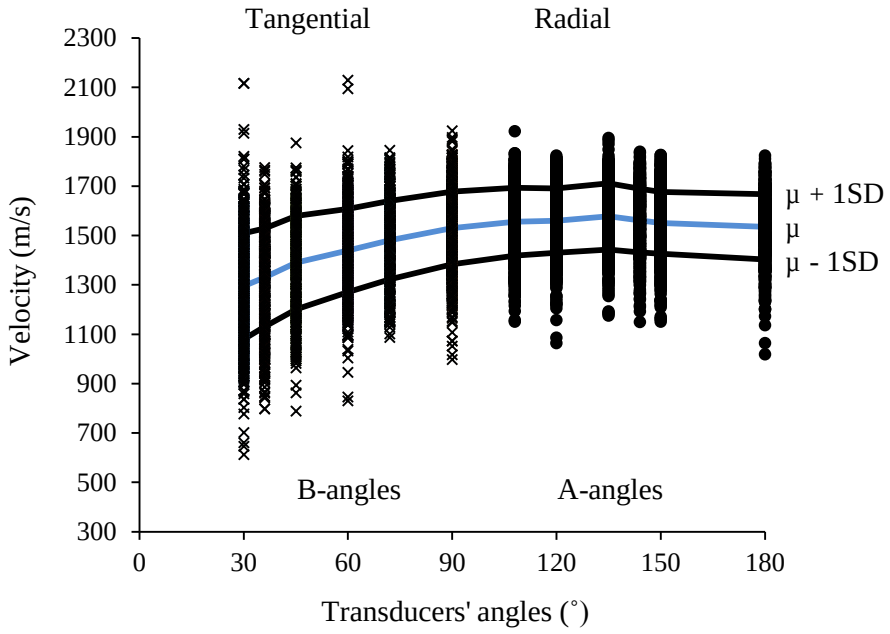


Figure 6. The reference velocity at different transducer angles of 25 sound discs

The measured velocities of 25 sound discs at the different transducers' angles are presented in Figure 6. The mean velocities at the smaller angles are slower than that at the larger angles as predicted because most of the stress wave paths at the smaller angles are closely orientated with the annual rings in tangential directions and most paths at the larger angles orientation with the annual rings are nearer to radial directions. The difference in velocity from 108˚ to 180˚ is quite small (about 1.72% in average). However, the velocity decreases significantly starting from the angle 90˚ to 30˚ (about 10% in average) as shown in Table 4.

Table 4. Measured mean velocity and standard deviation of each transducer angle

| Velocity | Transducers' angles (degree) | | | | | | | | | | | |
|---|---|---|---|---|---|---|---|---|---|---|---|---|
| | 30 | 36 | 45 | 60 | 72 | 90 | 108 | 120 | 135 | 144 | 150 | 180 |
| Mean (m/s) | 1295 | 1330 | 1390 | 1439 | 1481 | 1530 | 1556 | 1560 | 1578 | 1561 | 1551 | 1535 |
| SD* | 214 | 199 | 189 | 169 | 159 | 147 | 138 | 131 | 134 | 129 | 125 | 132 |
| μ+1SD | 1509 | 1528 | 1579 | 1608 | 1640 | 1677 | 1694 | 1691 | 1712 | 1690 | 1677 | 1667 |
| μ-1SD | 1081 | 1131 | 1201 | 1270 | 1322 | 1383 | 1419 | 1430 | 1444 | 1431 | 1426 | 1402 |
| R** | -16% | -13% | -9% | -6% | -3% | 0% | 1% | 2% | 3% | 2% | 1% | 0% |

SD* is the standard deviation

R** is the comparison of velocity difference at each angle with the mean velocity at 90˚.

## 4.2. Index development

### 4.2.1. Comparison of velocity difference within a cross-section (ADV)

In order to decide the presence of heart rots by ADV, threshold for ADV is necessary to be determined. However the ADV would be changed by changing the numbers of transducer. Based on reference velocity (clause 4.1), threshold was determined for each number of transducers. Threshold for each transducer number was determined to have consistent probability of correct detection as in table 5. The calculated mean ADVs, standard deviation and cumulative percentage of each 8, 10 and 12 transducers of 25 sound discs are shown in Table 5. The probability percentages for mean ADV with different standard deviations were calculated by normal distribution with cumulative percentages (Figure 7).

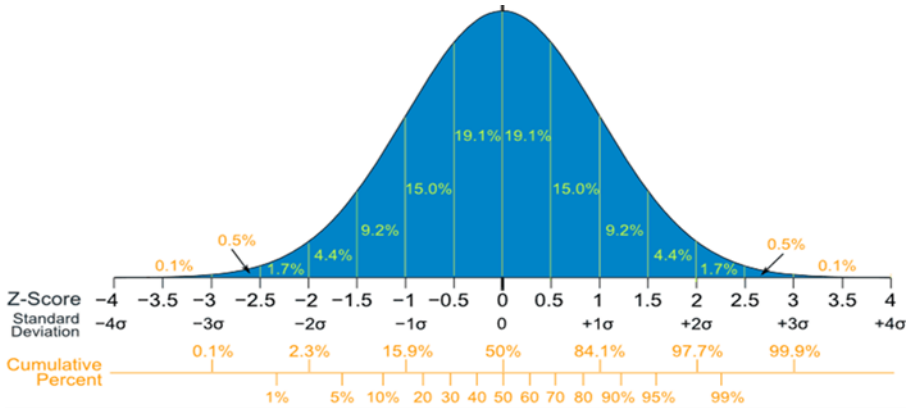


Figure 7. Normal distribution with percentages for every half of a standard deviation and cumulative percentages. ( *source: www.mathsisfun.com*)

Table 5. Mean ADV (%), standard deviation and cumulative percentages of 25 sound discs

| Probability | Z-score | ADV (%) for transducers no. | | |
|---|---|---|---|---|
| | | 8 | 10 | 12 |
| **50%** | **(μ)** | **-6.3** | **-9.5** | **-8.4** |
| 80% | (μ+0.84σ) | -5.46 | -8.66 | -7.56 |
| 85% | (μ+1.04σ) | -5.26 | -8.46 | -7.36 |
| 90% | (μ+1.28σ) | -5.02 | -8.22 | -7.12 |
| 95% | (μ+1.64σ) | -4.66 | -7.86 | -6.76 |
| 99% | (μ+2.33σ) | -3.97 | -7.17 | -6.07 |

The mean ADVs were found at (-6.3%) for 8 transducers, (-9.5%) for 10 transducers and (-8.4%) for 12 transducers. These results represent that the average mean velocities of B-angles are (6.3%), (9.5%) and (8.4%) slower than those of A-angles for 8, 10 and 12 transducer numbers respectively.

The mean ADV among each transducer number are different because transducer angles are different according the number of transducers used and velocities are different at different transducer angles. The velocity changes according to the angle between transducers are illustrated in Figures 8-a, 8- b and 8-c.

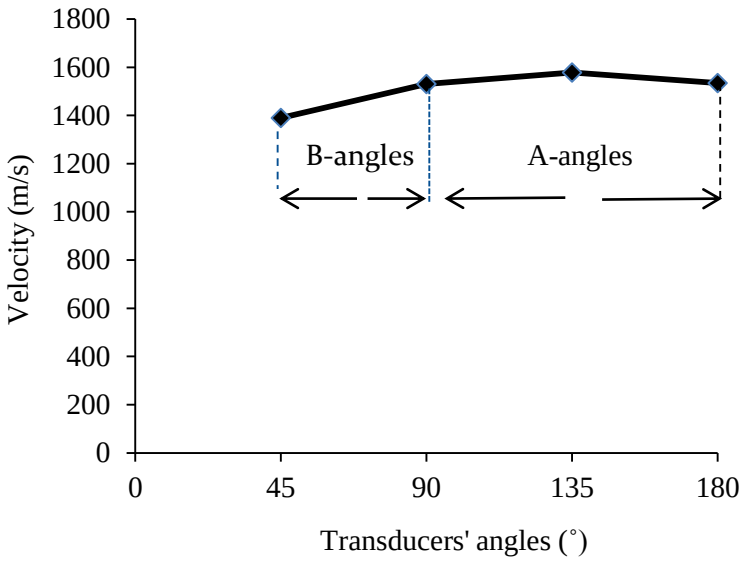


(a)

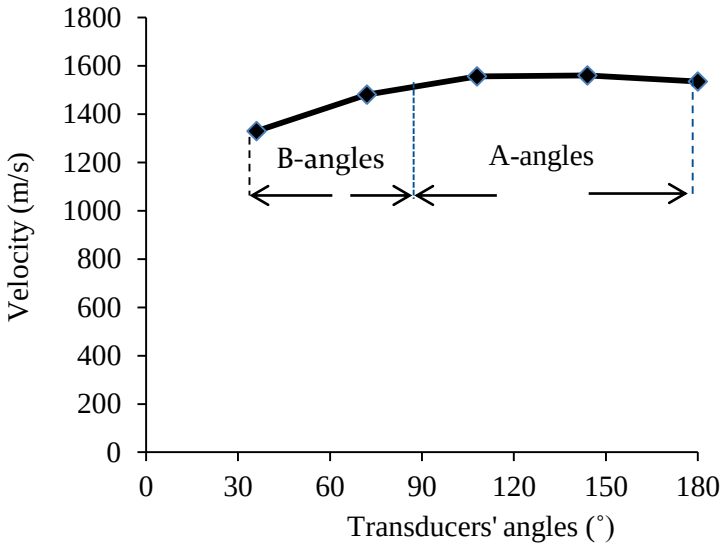


(b)

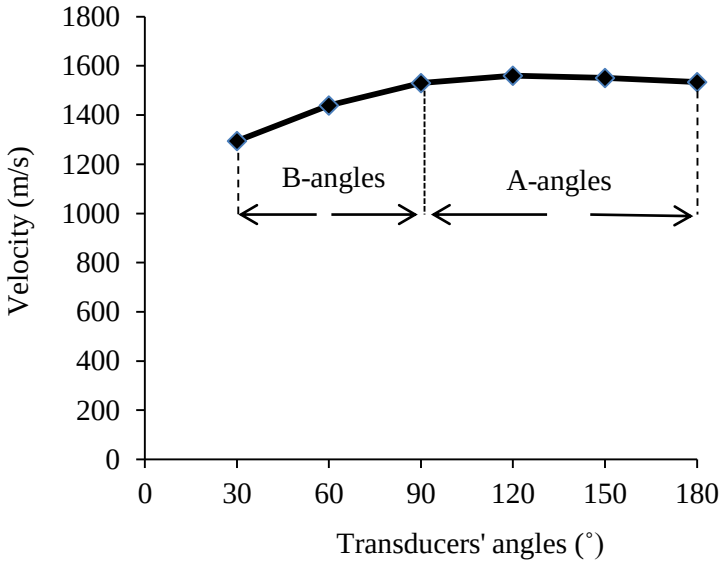


(c)

Figure 8. Different transducer numbers and their velocity changes from "B-angles" to "A-angles" for 25 sound discs with (a) 8 transducers, (b) 10 transducers and (c) 12 transducers.

In Table 6, the calculated ADVs for 10 sound and 9 defective discs are recorded. The result shows that the average ADV of sound discs is much smaller than that of defective discs. It indicates that the velocity of B-angle is quite slower than A-angle's velocity and the velocity difference is big in sound discs. In case of heart-rot discs, the velocity of B-angle is just a little slower and, sometimes, even faster than A-angle's velocity.

Table 6. Calculated ADV (%) for 10 sound discs and 9 defective discs with heart rots

| | Sound discs ADV | | | | Defective discs ADV | | |
|---|---|---|---|---|---|---|---|
| Disc no | No. of Transducers | | | Disc no | No. of Transducers | | |
| | 8 | 10 | 12 | | 8 | 10 | 12 |
| S1 | -7.3% | -10.9% | -9.4% | D1 | -5.1% | -7.2% | -6.4% |
| S2 | -5.7% | -7.5% | -9.6% | D2 | 0.4% | -1.3% | -1.0% |
| S3 | -10.1% | -10.4% | -10.6% | D3 | -5.3% | -7.4% | -7.7% |
| S4 | -7.8% | -12.2% | -9.1% | D4 | -0.8% | -3.0% | -3.0% |
| S5 | -11.6% | -15.9% | -13.8% | D5 | -4.6% | -4.0% | -4.3% |
| S6 | -7.0% | -9.1% | -9.0% | D6 | -1.1% | -3.8% | -2.7% |
| S7 | -11.2% | -12.8% | -12.9% | D7 | 7.5% | 4.0% | 5.9% |
| S8 | -5.8% | -7.0% | -8.0% | D8 | -3.2% | -4.9% | -4.2% |
| S9 | -10.5% | -10.9% | -11.9% | D9 | 14.2% | 9.9% | 13.5% |
| S10 | -6.5% | -9.7% | 8.9% | | | | |
| Average | **-8.4%** | **-10.6%** | **-8.5%** | | **0.2%** | **-2.0%** | **-1.1%** |

Based on the mean (μ) ADV of 25 reference sound discs and (μ±SD) standard deviation, calibration was carried out on these 10 sound and 9 defective discs' ADVs. After carried out calibration on 19 tested discs, the resulted threshold ADVs with the probability and accuracy percentages are tabled in Table 7, 8 and 9.

Table 7. The accuracy percentage and probabilities of indices with respect to standard deviations for 19 tested discs for 8 transducers

| Threshold | | | Accuracy for | | |
|---|---|---|---|---|---|
| Probability | z-score | ADV (%) | Total | Sound | Def. |
| 50% | (μ) | -6.3 | 89.5% | 80.0% | 100% |
| 80% | (μ+0.84σ) | -5.46 | 100% | 100% | 100% |
| 85% | (μ+1.04σ) | -5.26 | 94.7% | 100% | 88.9% |
| 90% | (μ+1.28σ) | -5.02 | 89.5% | 100% | 77.8% |
| 95% | (μ+1.64σ) | -4.66 | 89.5% | 100% | 77.8% |
| 99% | (μ+2.33σ) | -3.97 | 84.2% | 100% | 66.7% |

Table 8. The accuracy percentage and probabilities of indices with respect to standard deviations for 19 tested discs for 10 transducers

| Threshold | | | Accuracy for | | |
|---|---|---|---|---|---|
| Probability | z-score | ADV (%) | Total | Sound | Def. |
| 50% | (μ) | -9.5 | 84.2% | 70.0% | 100% |
| 80% | (μ+0.84σ) | -8.66 | 89.5% | 80.0% | 100% |
| 85% | (μ+1.04σ) | -8.46 | 89.5% | 80.0% | 100% |
| 90% | (μ+1.28σ) | -8.22 | 89.5% | 80.0% | 100% |
| 95% | (μ+1.64σ) | -7.86 | 89.5% | 80.0% | 100% |
| 99% | (μ+2.33σ) | -7.17 | 84.2% | 90.0% | 77.8% |

Table 9. The accuracy percentage and probabilities of indices with respect to standard deviations for 19 tested discs for 12 transducers

| Threshold | | | Accuracy for | | |
|---|---|---|---|---|---|
| Probability | z-score | ADV (%) | Total | Sound | Def. |
| 50% | (μ) | -8.4 | 94.7% | 90.% | 100.% |
| 80% | (μ+0.84σ) | -7.56 | 94.7% | 100% | 88.9% |
| 85% | (μ+1.04σ) | -7.36 | 94.7% | 100% | 88.9% |
| 90% | (μ+1.28σ) | -7.12 | 94.7% | 100% | 88.9% |
| 95% | (μ+1.64σ) | -6.76 | 94.7% | 100% | 88.9% |
| 99% | (μ+2.33σ) | -6.07 | 89.5% | 100% | 77.8% |

Table 10. The accuracy of indices with respect to standard deviation for 19 tested discs

| Transducer | Threshold | | | Accuracy for | | |
|---|---|---|---|---|---|---|
| no | z-score | Probability | ADV (%) | Total | Sound | Def. |
| 8 | μ+0.84 | 80% | -5.46 | 100% | 100% | 100% |
| 10 | μ+0.84 | 80% | -8.66 | 89.5% | 80% | 100% |
| 12 | μ+0.84 | 80% | -7.56 | 94.7% | 100% | 88.9% |

The best indices were found at (-5.46%) for 8 transducers, (-8.66%) for 10 transducers and (-7.56%) for 12 transducers (Table 10). According to the transducer numbers and their accuracy, it was found that the transducer quantity did not have significant influence on the accuracy of heart rot detection within a cross-section.

The developed indices are useful because tree inspector can easily identify the presence of decay of a tree by comparing the computed ADV of tested tree with the threshold ADV of each transducer number.

#### 4.2.1.1. Limitations of the ADV method

Development of indices was made on the basis of the velocity difference between inner zone and outer zone of a cross-section. Indices were developed based on an assumption that the velocity at outer zone "B-angles" is slower than the velocity at inner zone "A-angles" in a cross-section because of the anisotropic properties of wood. If the defect locates in the outer zone, the velocity of the outer zone will be much slower than that of the inner zone. ADV will be bigger indicating that the tree was sound although it was defective. Therefore, these indices can wrongly predict the internal condition of a tree if that has defects in the outer zone of a cross-section. Special care must be paid to check the outer surface of the bark before applying this method. It should not be applied to the trees which look like there is defect beneath the bark. In this study, the different ratios of heartwood and sapwood in each wood were not taken into consideration. The non-uniform orientation of annual rings because of uncertain pith location and non-circular shape of cross-sections of discs were ignored.

### 4.2.2. Comparison of tested discs' velocity with the reference velocity of sound discs (DIV)

#### 4.2.2.1. Calibration on the calculated DIVs of 10 sound discs and 9 heart-rot discs

Table 11. Accuracy of $DI_{a,a}$ index in distinguishing sound and defective discs

| No. of transducers | $DI_{a,a}$ | Accuracy (%) for | | |
|---|---|---|---|---|
| | | Sound | Decay | Overall |
| 8 | -0.2 | 63.6 | 54.5 | 59.1 |
| 10 | 0.2 | 45.5 | 72.7 | 59.1 |
| 12 | -0.1 | 45.5 | 45.5 | 45.5 |

Table 12. Accuracy of $DI_{a,n}$ index in distinguishing sound and defective discs

| No. of transducers | $DI_{a,n}$ | Accuracy (%) for | | |
|---|---|---|---|---|
| | | Sound | Decay | Overall |
| 8 | -0.5 | 54.5 | 63.6 | 59.1 |
| 10 | -0.7 | 72.7 | 54.5 | 63.6 |
| 12 | -0.7 | 54.5 | 54.5 | 54.5 |

Firstly, sound and heart-rot discs were distinguished by $DI_{a,a}$ and $Di_{a,n}$ indices (Table 11 and 12). These two indices were calculated by averaging all DIVs and negative DIVs of a cross-section. As the number of wave paths within a cross-section was big, there were a large number of calculated DIVs. In general, DIVs of the sound area of the cross-section might result positive and the heart-rotted area might give negative DIVs. Averaging all DIVs gives more generalized fact about heart rots than averaging only negative DIVs. By averaging only negative DIVs, $Di_{a,n}$ emphasizes more on heart rots' DIVs. Therefore, the overall accuracy of $Di_{a,n}$

is better than that of $DI_{a,a}$. Since $DI_{a,a}$ was calculated by averaging all DIVs, the impact of positive DIVs in sound part affected on the overall accuracy of distinguishing sound and heart-rot discs.

Table 13. Accuracy of $DI_{i,a}$ index in distinguishing sound and defective discs

| No. of transducers | $DI_{i,a}$ | Accuracy (%) for | | |
|---|---|---|---|---|
| | | Sound | Decay | Overall |
| 8 | -0.2 | 63.6 | 63.6 | 63.6 |
| 10 | 0.3 | 63.6 | 63.6 | 63.6 |
| 12 | -0.1 | 54.5 | 63.6 | 59.1 |

Table 14. Accuracy of $DI_{i,n}$ index in distinguishing sound and defective discs

| No. of transducers | $DI_{i,n}$ | Accuracy (%) for | | |
|---|---|---|---|---|
| | | Sound | Decay | Overall |
| 8 | -0.7 | 72.7 | 54.5 | 63.6 |
| 10 | -0.6 | 72.7 | 54.5 | 63.6 |
| 12 | -0.8 | 72.7 | 54.5 | 63.6 |

Accuracies of $DI_{i,a}$ and $DI_{i,n}$ are presented (Table 13 and 14). Averaging only DIVs of A-angle shows better result than $DI_{a,a}$ and $DI_{a,n}$ because the locations of heart rots of all tested discs are in the inner zone of cross-section. Among these four indices, the accuracy of $DI_{i,n}$ is better than others. $DI_{i,n}$ indices represent the inner zone of the cross-section and consider only on the velocity of wave paths which are slower than reference velocity of sound wave paths. Averaging DIVs of $DI_{i,n}$ are getting more different from sound disc's DIVs and giving better fact to distinguish sound and heart-rot discs.

### 4.2.2.2. Estimation of the sizes of heart rots in cross-section by *DI* indices

*DI* index has a meaning of how much the tested disc is different from sound discs. To explore the relationship between DI index and heart-rot's size, heart-rot area ratios of defective discs were measured. The calculated indices ($DI_{a,a}$, $DI_{a,n}$, $DI_{i,a}$ and $DI_{i,n}$) were used to analyze.

The defect area ratios of 9 heart rot discs are presented in Table 15.

The results of detection for the different defect area ratios are demonstrated in Figures 9, 10, 11 and 12.

Table 15. The defective area ratios of 9 heart-rot discs

| Disc. No | D1 | D2 | D3 | D4 | D5 | D6 | D7 | D8 | D9 |
|---|---|---|---|---|---|---|---|---|---|
| Defect Area Ratio (%) | 1.6 | 0.5 | 1.4 | 11.2 | 3.3 | 0.9 | 0.5 | 4.8 | 9.0 |

$DI_{a,a}$; Averaging all DIVs of the cross-section

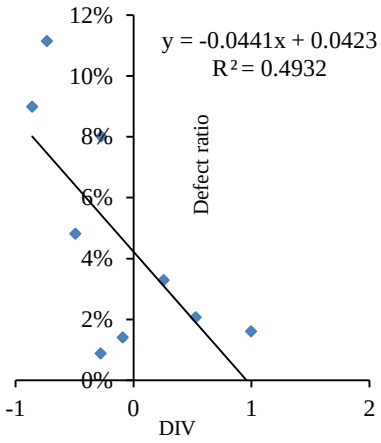


(a)

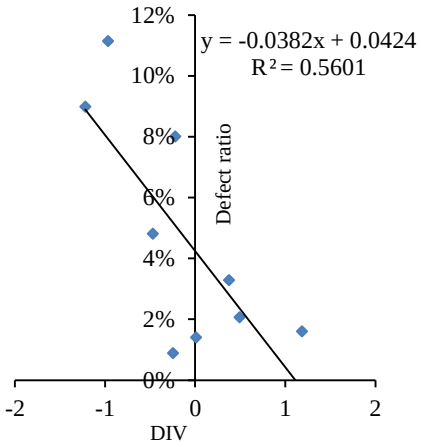


(b)

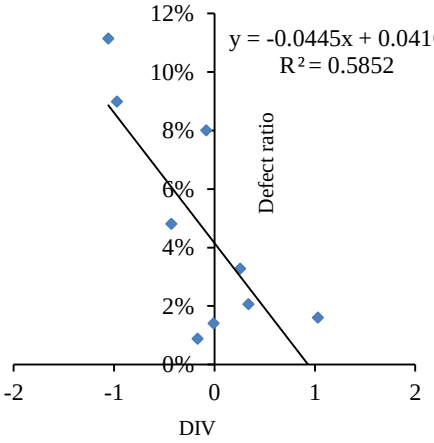


(c)

Figure 9. The area ratio of defects and DIV curve of the $DI_{a,a}$ indices for (a) 8 transducers (b) 10 transducers and (c) 12transducers

$DI_{a,n}$; Averaging negative DIVs of the cross-section

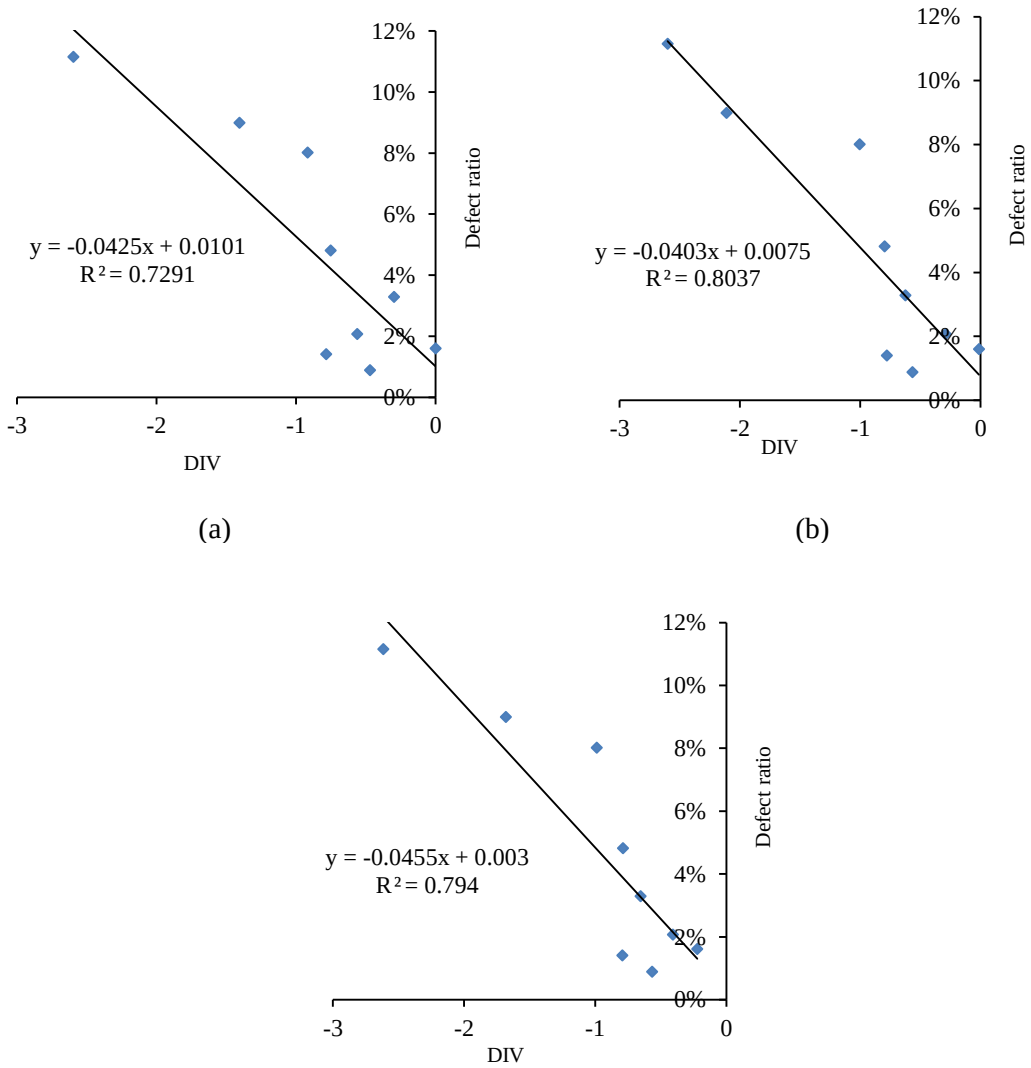


Figure 10. The area ratio of defects and DIV curve of the $DI_{a,n}$ indices for (a) 8 transducers (b) 10 transducers and (c) 12transducers

$DI_{i,a}$; Averaging all DIVs of the inner zone (A-angles) of the cross-section

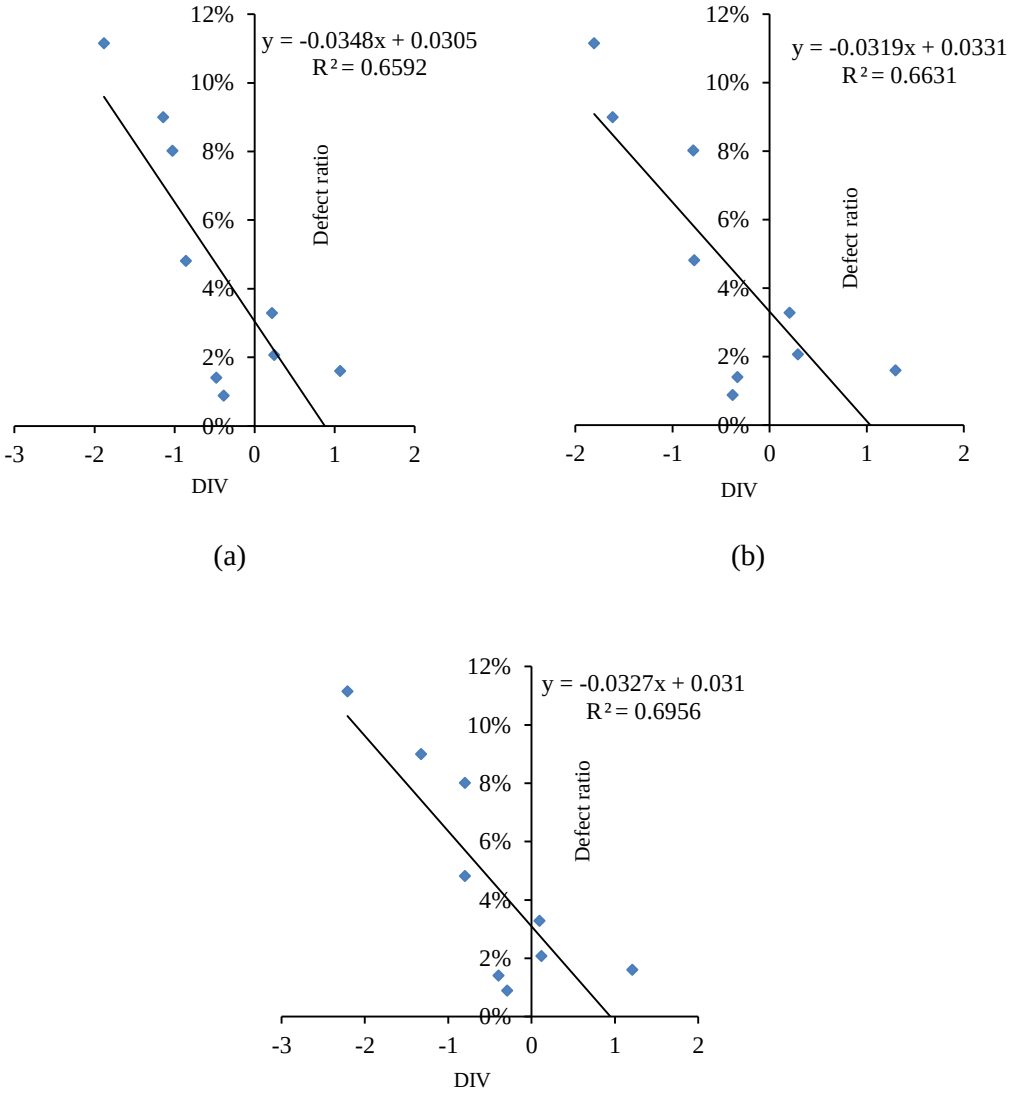


Figure 11. The area ratio of defects and DIV curve of the $DI_{i,a}$ indices for (a) 8 transducers (b) 10 transducers and (c) 12transducers

$DI_{i,n}$; Averaging negative DIVs of the inner zone (A-angles) of the cross-section

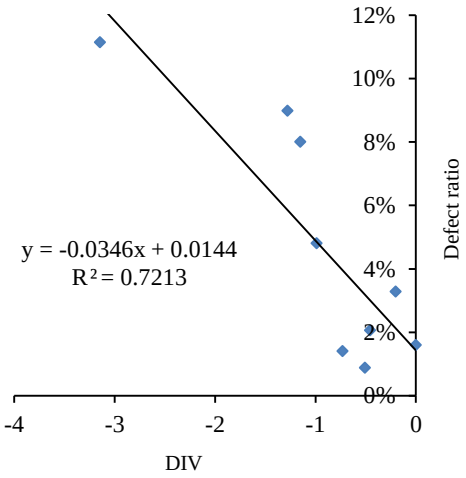


(a)

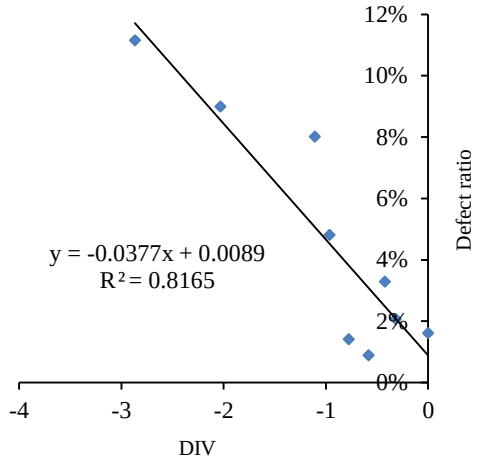


(b)

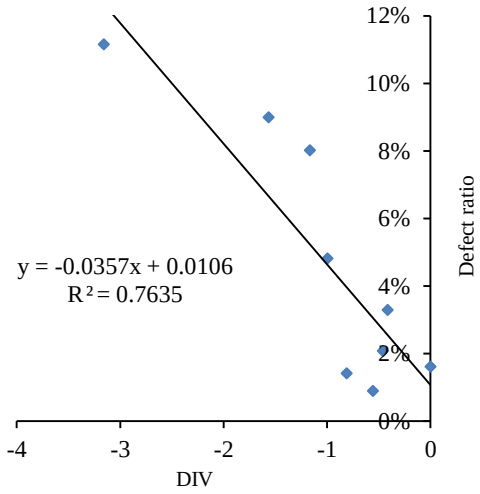


(c)

Figure 12. The area ratio of defects and DIV curve of the $DI_{i,n}$ indices for (a) 8 transducers (b) 10 transducers and (c) 12transducers

The regression analysis between the area ratios of heart rots and the feasibility of different indices with different transducer numbers are presented (Figures 9, 10, 11 and 12). Among them, $DI_{a,n}$ and $DI_{i,n}$ indices shows the better results than other indices because those two indices are calculated based on only negative DIVs. Only the DIVs of wave paths which velocities were slower than the reference velocity of sound data were taken into consideration.

Although $DI_{i,a}$ index emphasizes on DIVs of the inner zone of cross-section where heart rots exist, its relationship with heart-rot's area ratio is still weaker than $DI_{a,n}$. This result points out that the positive DIVs have impact on estimating the area ratios of heart rots. This analysis indicates that there is a good relationship with the decay area ratio in the cross-section and calculated DIVs. These DIVs' indices can be used to predict the sizes of heart rots in the cross-sections of teak trees.

## 5. CONCLUSIONS

This study was carried out to develop less complex indices which can be used as additional decision-making criteria in detecting heart rots while using stress wave CT instruments.

The followings were concluded from this study.

1. The velocity change pattern from “B” to “A” angles is one of the important indicators to detect heart rot in Teak.
2. The visible outer part of the stem needs to be carefully checked. The existence of any kind of decay on the tree stem can affect the ADV calculation and lead to wrong decision making.
3. The defective area ratio of the cross-section can be predicted by using dissimilarity values calculated by comparing the measured velocity with the reference velocity (DIVs) of sound discs.
4. The developed indices can be used additionally as decision making criteria to detect heart rots while using the stress wave CT devices.

## 6. REFERENCES

Bucur,V. (1999). Acoustics as a tool for the nondestructive testing of wood. International symposium on NDT contribution to the infrastructure safety system, 1999 NOV 22-26.

Dackermann, U., K.Crews, B.Kasal, J.Li, M.Riggio, F.Rinn and T.Tannert. (2013). In situ assessment of structural timber using stress-wave measurements. Materials and Structures, DOI 10.1617/s 11527-013-0095-4, original article.

Dikrallah,A., B.Kabouchi, A.Hakam, L.Brancheriau, H.Bailleres. , A.Famiri and M.Ziani. (2010). Study of acoustic wave propagation through the cross-section of green wood. C. R. Mecanique 338 (2010) 107-112.

Divos, F. and L. Sazlai. (2002). Tree evaluation by acoustic tomography. In: Proceedings of the 13th international Symposium on Nondestructive Testing of Wood, August 19-21, 2002, Berkeley, California. pp. 251-256.

Divos, F. and Divos.P. (2005). Resolution of stress wave based acoustic tomography. In: Proceedings of the 14th International Symposium on Nondestructive Testing of Wood, May 2-4, 2005, University of Applied Sciences, Eberswalde, Germany; Shaker Verlag, Eberswalde, Germany. pp. 309-314.

Gao, S., Wang.X, Wang.L, Allison. R.B. (2012). Effect of temperature on acoustic evaluation of standing trees and logs: Part 2: Field investigation. Wood and

Fiber Science, 45(1), 2013, pp. 1-11. Society of Wood Science and Technology.

Gyi, M. K. K. (1972). An investigation of factors relevant to development of teak plantations in South East Asia with particular reference to Burma. M.Sc Thesis. Australia National University (ANU). Canberra, Australia.

Halabe, U.B, BIIMgalu. G.M, GangaRao. H.V.S and Ross.R.J. (1995). Nondestructive evaluation of green wood using stress wave and transverse vibration techniques. Materials Evaluation, Vol.55, No.9, pp. 1013-1018.

Hlaing, Z. C. (2012). The growth of Teak (*Tectona grandis* Linn.f) in different aged plantations in Bago Yoma range, Myanmar. M.Sc Thesis. Seoul National University, Seoul, Republic of Korea.

Htun, K. and C. Hlaing. (2001). A general assessment of teak plantations in the Bago Yoma Region, Yangon, Myanmar: FRI Leaflet No.8. Forest Science Research Paper, Forest Department.

Johnstone, D, Moore. G, Tausz. M, Nicolas. M. (2010). The measurement of wood decay in landscape trees. Arboriculture & Urban Forestry 36(3): 121-127.

Krishnapillay, B. (2000). Silviculture and Management of teak plantations. Unasylva, 51: 14-21.

Kyaw, N. N. (2003). Site Influence on Growth and Phenotype of Teak (*Tectonal grandis* Linn.f) in Natural Forests of Myanmar. Ph. D Thesis. Germany: Cuvillier Verlag, Gottingen.

Kim, K.M. (2005). Algorithm development of ultrasonic CT for detecting wood deterioration by emphasizing on the effects of wood anisotropy and

ultrasound diffraction. Ph. D Thesis. Republic of Korea: Dept. Forest Sciences. Seoul National University.

Ladrach, W. (2009). Management of teak plantations for solid wood products, Bethsda, Maryland 20814, USA.

Li, G., X. Wang, J. Wiedenbeck and R.J.Ross. (2013). Analysis of wave velocity patterns in Black Cherry trees and its effect on internal decay detection. Proceedings 18th international Nondestructive Testing and Evaluation of Wood Symposium, Madison, Wisconsin, USA.2013.

Liang, S., F.Fu, L.Lin, N.Hu. (2010). Various factors and propagation trends of stress waves in cross sections of Euphrates Poplar. Forest Products Journal.

Liang, S., F.Fu. (2012). Relationship analysis between tomograms and hardness maps in determining internal defects in Euphrates Poplar. Chinese Academy of Forestry, Research Institute of Wood Industry, Beijing, China. Wood Research, 57 (2):2012, 221-230.

Li-hai., Wang, X.Hua-dong, Z.Ci-lin, L.Li, and Y.Xue-chun. (2000). Effect of sensor quantity on measurement accuracy of log inner defects by using stress wave.Journal of Forestry Research (Harbin) 18(3):221-225.

Lin, C.J., Kao. Y.C, Lin. T.T, Tsai. M.J, Wang. S.Y, Lin. L.D, Wang. Y.N and Chan. M.H. (2008). Application of an ultrasonic tomographic technique for detecting defects in standing trees. International biodeterioration & biodegradation 62 (2008) 434-441.

Luo, J., Yang.X. (2010). Experimental research on different propagation velocity of stress wave in Poplar and Larch logs. 2010 International Conference on Computer, Mechatronics, Control and Electronic Engineering (CMCE).

Martin, P.A., Berger.J.R. (2000). Waves in wood: free vibrations of a wooden pole. Journal of Mechanics and Physics of Solids, 49 (2001) 1155-1178.

Pellerin, R.F. and R.J. Ross. (2002). Nondestructive Evaluation of Wood. Forest Products Society, Madison, Wisconsin, USA.

Soe, K. K. (2009). Growth performance of Teak (*Tectona grandis* Linn.f) plantations in moist and dry ecological zones in Myanmar. M.Sc Thesis. University of Technology, Dresden. Germany.

Suhaendi, Hendi. 1998. Teak improvement in Indonesia. In: Teak for the Future, Proceedings of the Second Regional Seminar on Teak, 29 May - 3 June 1995, Yangon, Myanmar. FAO Regional Office for Asia and the Pacific (RAP) Bangkok, Thailand RAP publication 1998/5.

Tallavo, F., G.Cascante and M.D.Pandey. (2012). A novel methodology for condition assessment of wood poles using ultrasonic testing, NDT&E international Vol.52, Pages 149-156.

Wang, X., F. Divos, C. Pilon, B.K. Brashaw, R.J. Ross, R.F. Pellerin. (2004). Assessment of decay in standing timber using stress wave timing nondestructive evaluation tools – A guide for use and interpre-tation. Gen. Tech. Rep. FPL –GTR–147. .S. Department of Agri-culture, Forest Service, Forest Products Laboratory, Madison, WI. 12.

Wang, X., J. R. Ross, and P. Carter. 2005. Acoustic evaluation of standing trees-resent research development. In: Proceedings of the 14th International Symposium on Nondestructive Testing of Wood, May 2-4, 2005, University of Applied Sciences, Eberswalde, Germany; Shaker Verlag, Eberswalde, Germany. pp. 455-465.

Wang, X., Wiedenbeck, J., Ross, R.J., Forsman, J.W., Erickson, J.R., Pilon, C. and Brashaw, B.K. (2005). Nondestructive evaluation of incipient decay in hardwood logs. Gen. Tech. Rep. FPL-GTR-162, Madison, WI: U.S. Department of Agriculture, Forest Service, Forest Products Laboratory, 11p.

Wang, X., P. Carter, R.J. Ross, B.K. Brashaw. (2007). Acoustic assessment of wood quality of raw forest materials -A path to increased profitability. Forest Product Journal 57(5): 6-14.

Wang, X., R. Bruce Allison. (2008). Decay detection in Red Oak using a combination of visual inspection, acoustic testing, and resistance microdrilling, Arboriculture & Urban Forestry 34(1).

Yamamoto, Koichi, Sulaiman, Othman, Hashim, Rokiah. (1998). Nondestructive detection of heart rot in Acacia mangium trees in Malaysia, Forest Products Journal, Vol.48 Issue 3, p83.

## ABSTRACT IN KOREA


티크(Teak)는 강도, 매력적인 목리 패턴, 흰개미에 대한 저항성, 내구성과 쾌적한 색상으로 유명하다. 지난 수 십년 동안 미얀마의 티크 천연림은 외국으로의 수출을 위한 벌채, 불법 벌목, 인구과잉으로 인한 수요량 증가 및 과다 사용 등으로 감소되었다. 티크 천연림의 감소를 방지하면서 요구되는 티크를 지속적으로 공급하고자, 미얀마 정부는 전 국가에 걸쳐 티크 조림지를 조성하였다. 티크 조림지의 목적은 티크의 공급량을 지속적으로 유지하면서 목재의 품질을 유지하는 것이다.

성공적인 조림지 조성을 위해서는 간벌작업이 필수적이다. 조림지에서 일부 입목을 제거함으로써 남은 입목은 더 많은 햇빛과 영양소를 공급받을 수 있으며, 입목간의 강한 경쟁이 완화될 수 있기 때문이다. 간벌작업에 있어서, 벌채할 입목을 선정하는 작업은 특별한 주의가 요구된다. 건전한 입목을 베어내고 결함이 있는 입목을 남겨두는 것은 경제적으로 큰 손실을 초래하기 때문이다. 육안 검사는 심재부후(heart rot)와 같은 입목 내부에 있는 결함을 탐지할 수 없다. 응력파 CT 기기에 의한 단층촬영(tomograph)은 입목의 단

면이미지를 획득할 수 있지만, 단면이미지를 분석하여 입목의 정확한 상태를 판단하기 위해서는 많은 경험이 축적되어야 한다. 판단의 오류를 방지하기 위해서는 응력파 CT 기기를 사용하여 내부결함의 존재 여부를 판단할 수 있는 추가적인 기준이 필요하다. 본 연구의 목적은 심재부후의 존재 여부를 판단할 수 있는 기준을 개발하는 것이다.

응력파 CT 기술을 적용하여 입목을 탐지할 때, 여러 개의 트랜스듀서(transducer)를 입목 둘레에 고정한다. 트랜스듀서 8개, 10개, 12개를 사용하여 트랜스듀서 사이의 응력파 전달 시간(the time of flight)을 측정하였다. 트랜스듀서 사이의 각도는 단면을 가로지르는 선(180°)을 기준으로 정의되었다. 트랜스듀서 8개, 10개, 12를 사용하였을 때 각각 4개의 각도(30°, 90°, 120°, 180°), 5개의 각도(36°, 72°, 108°, 144°, 180°), 6개의 각도(30°, 60°, 90°, 120°, 150°, 180°)가 정의된다. 건전한 시험편 (sound discs) 25개를 사용하여 트랜스듀서의 각도에 대한 기준속도(reference velocity)를 도출하였다. 심재부후는 입목의 중앙부 근처에서 발생하기 때문에, 트랜스듀서 사이의 각도를 기준으로 단면을 외부영역(outer zone)와 내부영역(inner zone) 두

부분으로 나누었다. 외부영역은 90°보다 작거나 같은 각도를 포함하고, 내부영역은 90°보다 큰 각도를 포함한다.

건전한 시험편 25개의 시험결과, 외부영역을 통과하는 응력파의 속도가 내부영역을 통하는 응력파의 속도보다 느렸다. 이것은 90°보다 작은 각도는 접선방향에 있는 연륜(annual ring)과 방향이 유사하고, 90°보다 큰 각도는 접선뱡항에 가깝기 때문이다. 우선, 건전한 시험편 25개의 내부영역과 외부영역의 평균 속도를 분석한 후 트랜스듀서의 개수에 따라 각 시험편마다 두 영역 사이의 ADV (Average Difference Velocity, %) index를 계산하였다. 기준치(reference)는 건전한 25개 시험편의 ADV index를 의미하며 8개, 10개, 12개의 트랜스듀서를 사용하였을 때 각각 -6.26%, -9.53%, -8.35%로 결정되었다.

건전한 시혐편 (sound disc) 10개와 심재가 부후된 시험편 (heart-rot disc) 9개를 대상으로 같은 실험을 수행하였다. 건전한 시험편 10개의 ADV index 범위는 8개, 10개, 12개의 트랜스듀서를 사용하였을 때 각각 (-8.61% ~ -15.25%), (-5.7% ~ -11.62), (-6.97% ~ -15.94%)로 나타났다. 심재가 부후된

시험편 9개의 ADV index범위는 8개, 10개, 12개의 트랜스듀서를 사용하였을 때 각각 (10.68% ~ -8.38%), (14.2% ~ -5.26), (9.93% ~ -7.4%)로 나타났다. 심재부후는 단면의 중심부에 위치하기 때문에, 외부영역의 평균속도는 결함이 있는 시험편의 내부영역의 평균속도보다 조금 느리거나 훨씬 빨랐다. 측정된 19개 시험편의 ADV index를 기준치 ADV index와 비교하였을 때, 건전한 시험편과 심재가 부후된 시험편이 높은 정확도(89.5~100%)로 구분되었다.

건전한 시험편(10개)와 심재가 부후된 시험편(9개)에서 측정된 속도를 각도별 기준속도(reference velocity)와 비교하였다. 그리고 기준속도와 얼마나 차이가 있는지에 대한 DIV (Dissimilarity in Velocity) index를 계산하였다. 모든 각도에서의 평균±DIV index와 19개 시험편의 내부영역에 해당하는 각도를 기준으로 건전한 시험편과 심재부후 시험편을 구분하였다. 비록 심재부후 탐지 정확도는 59.1-63.6%로 높지 않았지만 단면에 있는 심재부후의 면적 비율과 계산된 DIV index 사이에는 선형관계가 있었다. 결론적으로 응력파 CT 영상기기를 사용하여 심재부후를 탐지할 때, 본 연구에서 적용한

두 기준치(ADV index, DIV index)를 심재부후 탐지 및 면적비율 예측을 위한 의사결정 기준으로 사용할 수 있을 것으로 사료된다.

# APPENDICES

## A-1. Average Difference Velocity (ADV %) of 25 sound discs

| | ADV for different transducer number | | |
|---|---|---|---|
| Disc no. | 8 | 10 | 12 |
| 1 | -10.60% | -14.25% | -12.60% |
| 2 | -10.27% | -14.17% | -12.42% |
| 3 | -8.83% | -14.11% | -11.24% |
| 4 | -4.50% | -8.25% | -8.01% |
| 5 | -10.27% | -16.54% | -13.59% |
| 6 | -10.54% | -14.64% | -13.33% |
| 7 | -8.93% | -15.54% | -11.77% |
| 8 | -13.47% | -16.08% | -15.92% |
| 9 | -4.99% | -9.82% | -8.59% |
| 10 | -5.37% | -7.06% | -7.98% |
| 11 | -4.04% | -5.94% | -4.94% |
| 12 | -3.94% | -7.75% | -5.20% |
| 13 | 0.20% | -4.49% | -2.14% |
| 14 | -5.17% | -7.35% | -6.88% |
| 15 | -8.83% | -9.77% | -10.62% |
| 16 | -1.52% | -3.71% | -2.55% |
| 17 | -4.03% | -7.75% | -5.98% |
| 18 | -3.72% | -5.22% | -5.29% |
| 19 | -0.56% | -5.35% | -2.51% |
| 20 | -4.31% | -6.52% | -6.30% |
| 21 | -5.19% | -8.34% | -6.20% |
| 22 | -5.26% | -7.06% | -7.44% |
| 23 | -3.83% | -5.53% | -5.89% |
| 24 | -7.84% | -9.05% | -10.04% |
| 25 | -10.77% | -13.90% | -11.30% |

**A-2. The defect ratios of heart-rot discs and their calculated *DI* indices**

| Defect ratio | $DI_{a,a}$ | | | $DI_{a,n}$ | | | $DI_{i,a}$ | | | $DI_{i,n}$ | | |
|---|---|---|---|---|---|---|---|---|---|---|---|---|
| | Number of transducers | | | | | | | | | | | |
| | 8 | 10 | 12 | 8 | 10 | 12 | 8 | 10 | 12 | 8 | 10 | 12 |
| 0.5% | -0.64 | -0.79 | -0.77 | -1.51 | -1.46 | -1.53 | -1.24 | -1.28 | -1.38 | -1.58 | -1.68 | -1.75 |
| 0.5% | 0.14 | 0.09 | 0.50 | -0.34 | -0.34 | -0.38 | 0.28 | 0.08 | 0.63 | -0.27 | -0.36 | -0.17 |
| 0.9% | -0.28 | -0.25 | -0.17 | -0.47 | -0.57 | -0.56 | -0.39 | -0.38 | -0.29 | -0.51 | -0.58 | -0.56 |
| 1.4% | -0.09 | 0.01 | -0.01 | -0.78 | -0.78 | -0.79 | -0.48 | -0.33 | -0.40 | -0.73 | -0.78 | -0.81 |
| 1.6% | 1.00 | 1.18 | 1.03 | 0.00 | -0.01 | -0.22 | 1.07 | 1.30 | 1.21 | 0.00 | 0.00 | 0.00 |
| 2.1% | 0.53 | 0.49 | 0.34 | -0.56 | -0.29 | -0.41 | 0.25 | 0.29 | 0.12 | -0.46 | -0.32 | -0.46 |
| 3.3% | 0.26 | 0.38 | 0.26 | -0.30 | -0.63 | -0.65 | 0.22 | 0.21 | 0.10 | -0.20 | -0.42 | -0.41 |
| 4.8% | -0.49 | -0.47 | -0.43 | -0.75 | -0.80 | -0.79 | -0.86 | -0.77 | -0.80 | -0.99 | -0.97 | -1.00 |
| 8.0% | -0.27 | -0.22 | -0.08 | -0.92 | -1.01 | -0.99 | -1.03 | -0.78 | -0.80 | -1.15 | -1.11 | -1.17 |
| 9.0% | -0.86 | -1.22 | -0.97 | -1.41 | -2.11 | -1.68 | -1.14 | -1.61 | -1.33 | -1.28 | -2.03 | -1.57 |
| 11.2% | -0.73 | -0.97 | -1.06 | -2.60 | -2.60 | -2.61 | -1.88 | -1.81 | -2.21 | -3.15 | -2.87 | -3.16 |

**A-3. The mean velocity at different transducer's angles of 25 sound discs**

| Disc no. | | Transducers' angle (˚) | | | | | | | | | | | |
|---|---|---|---|---|---|---|---|---|---|---|---|---|---|
| | | 30 | 36 | 45 | 60 | 72 | 90 | 108 | 120 | 135 | 144 | 150 | 180 |
| 1 | Velocity (m/s) | 1169 | 1183 | 1229 | 1322 | 1381 | 1436 | 1486 | 1500 | 1490 | 1510 | 1502 | 1490 |
| 2 | | 1162 | 1184 | 1303 | 1334 | 1368 | 1454 | 1462 | 1494 | 1563 | 1489 | 1507 | 1509 |
| 3 | | 1186 | 1176 | 1254 | 1374 | 1372 | 1472 | 1478 | 1535 | 1510 | 1493 | 1528 | 1479 |
| 4 | | 1146 | 1250 | 1323 | 1328 | 1422 | 1460 | 1498 | 1456 | 1511 | 1468 | 1417 | 1403 |
| 5 | | 1023 | 1043 | 1168 | 1213 | 1243 | 1344 | 1356 | 1385 | 1424 | 1377 | 1383 | 1376 |
| 6 | | 1004 | 1043 | 1111 | 1196 | 1227 | 1291 | 1314 | 1340 | 1343 | 1334 | 1346 | 1342 |
| 7 | | 1073 | 1064 | 1193 | 1272 | 1278 | 1388 | 1380 | 1427 | 1446 | 1391 | 1416 | 1388 |
| 8 | | 1070 | 1120 | 1111 | 1271 | 1307 | 1343 | 1412 | 1442 | 1376 | 1466 | 1478 | 1461 |
| 9 | | 1103 | 1173 | 1232 | 1309 | 1363 | 1408 | 1448 | 1436 | 1430 | 1423 | 1395 | 1348 |
| 10 | | 1428 | 1544 | 1592 | 1557 | 1660 | 1674 | 1727 | 1673 | 1738 | 1731 | 1678 | 1713 |
| 11 | | 1448 | 1479 | 1496 | 1563 | 1604 | 1660 | 1676 | 1683 | 1704 | 1655 | 1645 | 1585 |
| 12 | | 1527 | 1488 | 1543 | 1642 | 1641 | 1710 | 1712 | 1748 | 1724 | 1714 | 1736 | 1662 |
| 13 | | 1420 | 1406 | 1503 | 1541 | 1545 | 1606 | 1580 | 1596 | 1588 | 1541 | 1557 | 1514 |

| Disc no. | | Transducers' angle (˚) | | | | | | | | | | | |
|---|---|---|---|---|---|---|---|---|---|---|---|---|---|
| | | 30 | 36 | 45 | 60 | 72 | 90 | 108 | 120 | 135 | 144 | 150 | 180 |
| 14 | velocity (m/s) | 1419 | 1455 | 1491 | 1539 | 1569 | 1607 | 1629 | 1637 | 1636 | 1635 | 1634 | 1632 |
| 15 | | 1348 | 1428 | 1447 | 1471 | 1539 | 1553 | 1614 | 1597 | 1629 | 1659 | 1633 | 1661 |
| 16 | | 1368 | 1393 | 1421 | 1512 | 1537 | 1538 | 1578 | 1568 | 1553 | 1536 | 1515 | 1451 |
| 17 | | 1428 | 1436 | 1511 | 1542 | 1575 | 1623 | 1647 | 1650 | 1662 | 1645 | 1632 | 1603 |
| 18 | | 1524 | 1591 | 1610 | 1639 | 1692 | 1718 | 1752 | 1735 | 1753 | 1741 | 1714 | 1704 |
| 19 | | 1453 | 1432 | 1532 | 1570 | 1563 | 1640 | 1618 | 1642 | 1646 | 1586 | 1597 | 1544 |
| 20 | | 1432 | 1479 | 1534 | 1558 | 1615 | 1639 | 1665 | 1659 | 1683 | 1666 | 1648 | 1634 |
| 21 | | 1444 | 1431 | 1510 | 1530 | 1577 | 1625 | 1642 | 1636 | 1669 | 1643 | 1630 | 1637 |
| 22 | | 1312 | 1382 | 1379 | 1447 | 1520 | 1532 | 1591 | 1572 | 1561 | 1582 | 1552 | 1511 |
| 23 | | 1246 | 1328 | 1368 | 1339 | 1420 | 1426 | 1470 | 1425 | 1483 | 1470 | 1416 | 1423 |
| 24 | | 1286 | 1385 | 1459 | 1392 | 1498 | 1510 | 1562 | 1517 | 1622 | 1592 | 1538 | 1600 |
| 25 | | 1353 | 1351 | 1435 | 1512 | 1505 | 1596 | 1611 | 1649 | 1699 | 1666 | 1682 | 1698 |